10
Turbulent-viscosity models

In this chapter and the next we consider RANS models in which the Reynolds equations are solved for the mean velocity field. The Reynolds stresses – which appear as unknowns in the Reynolds equations – are determined by a turbulence model, either via the turbulent viscosity hypothesis or more directly from modelled Reynolds-stress transport equations (Chapter 11).

Turbulent-viscosity models are based on the turbulent-viscosity hypothesis, which was introduced in Chapter 4 and has been used in subsequent chapters. According to the hypothesis, the Reynolds stresses are given by

$$\langle u_i u_j \rangle = \tfrac{2}{3} k \delta_{ij} - \nu_T \left(\frac{\partial \langle U_i \rangle}{\partial x_j} + \frac{\partial \langle U_j \rangle}{\partial x_i} \right), \tag{10.1}$$

or, in simple shear flow, the shear stress is given by

$$\langle uv \rangle = -\nu_T \frac{\partial \langle U \rangle}{\partial y}. \tag{10.2}$$

Given the turbulent viscosity field $\nu_T(\boldsymbol{x}, t)$, Eq. (10.1) provides a most convenient closure to the Reynolds equations, which then have the same form as the Navier–Stokes equations (Eq. (4.46) on page 93). It is unfortunate, therefore, that for many flows the accuracy of the hypothesis is poor. The deficiencies of the turbulent-viscosity hypothesis – many of which have been mentioned above – are reviewed in Section 10.1.

If the turbulent-viscosity hypothesis is accepted as an adequate approximation, all that remains is to determine an appropriate specification of the turbulent viscosity $\nu_T(\boldsymbol{x}, t)$. This can be written as the product of a velocity $u^*(\boldsymbol{x}, t)$ and a length $\ell^*(\boldsymbol{x}, t)$:

$$\nu_T = u^* \ell^*, \tag{10.3}$$

and the task of specifying ν_T is generally approached through specifications of u^* and ℓ^*. In algebraic models (Section 10.2) – the mixing-length model,

for example – ℓ^* is specified on the basis of the geometry of the flow. In two-equation models (Section 10.4) – the k-ε model being the prime example – u^* and ℓ^* are related to k and ε, for which modelled transport equations are solved.

10.1 The turbulent-viscosity hypothesis

The turbulent-viscosity hypothesis can be viewed in two parts. First, there is the *intrinsic* assumption that (at each point and time) the Reynolds-stress anisotropy $a_{ij} \equiv \langle u_i u_j \rangle - \frac{2}{3}k\delta_{ij}$ is determined by the mean velocity gradients $\partial\langle U_i \rangle / \partial x_j$. Second, there is the *specific* assumption that the relationship between a_{ij} and $\partial\langle U_i \rangle / \partial x_j$ is

$$\langle u_i u_j \rangle - \tfrac{2}{3}k\delta_{ij} = -\nu_T \left(\frac{\partial \langle U_i \rangle}{\partial x_j} + \frac{\partial \langle U_j \rangle}{\partial x_i} \right), \tag{10.4}$$

or, equivalently,

$$a_{ij} = -2\nu_T \bar{S}_{ij}, \tag{10.5}$$

where $\bar{S}_{ij}$ is the mean rate-of-strain tensor. This is, of course, directly analogous to the relation for the viscous stress in a Newtonian fluid:

$$-(\tau_{ij} + P\delta_{ij})/\rho = -2\nu S_{ij}. \tag{10.6}$$

10.1.1 The intrinsic assumption

To discuss the intrinsic assumption we first describe a simple flow for which it is entirely incorrect. Then it is shown that, in a crucial respect, the physics of turbulence is vastly different than the physics of the molecular processes that lead to the viscous stress law (Eq. (10.6)). However, finally, it is observed that, for simple shear flows, the turbulent viscosity hypothesis is nevertheless quite reasonable.

Axisymmetric contraction

Figure 10.1 is a sketch of a wind-tunnel experiment, first performed by Uberoi (1956), to study the effect on turbulence of an axisymmetric contraction. The air flows through the turbulence-generating grid into the first straight section, in which the mean velocity $\langle U_1 \rangle$ is (ideally) uniform. In this section there is no mean straining ($\bar{S}_{ij} = 0$), and the turbulence (which is almost isotropic) begins to decay.

Following the first straight section there is an axisymmetric contraction, which is designed to produce a uniform extensive axial strain rate,

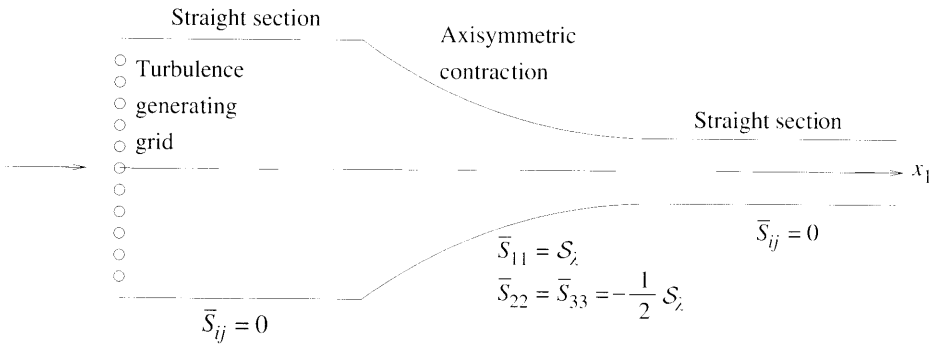

Fig. 10.1. A sketch of an apparatus, similar to that used by Uberoi (1956) and Tucker (1970), to study the effect of axisymmetric mean straining on grid turbulence.

$\bar{S}_{11} = \partial\langle U_1\rangle/\partial x_1 = \mathcal{S}_\epsilon$, and hence uniform compressive lateral strain rates, $\bar{S}_{22} = \bar{S}_{33} = -\frac{1}{2}\mathcal{S}_\epsilon$. The quantity $\mathcal{S}_\epsilon k/\varepsilon$ (evaluated at the beginning of the contraction) measures the mean strain rate relative to the turbulence timescale. Figure 10.2 shows measurements of the normalized anisotropies ($b_{ij} \equiv \langle u_i u_j\rangle/\langle u_k u_k\rangle - \frac{1}{3}\delta_{ij} = \frac{1}{2}a_{ij}/k$) from the experiment of Tucker (1970) with $\mathcal{S}_\epsilon k/\varepsilon = 2.1$. Also shown in Fig. 10.2 are DNS results for $\mathcal{S}_\epsilon k/\varepsilon = 55.7$ obtained by Lee and Reynolds (1985). For this large value of $\mathcal{S}_\epsilon k/\varepsilon$, rapid-distortion theory (RDT, see Section 11.4) accurately describes the evolution of the Reynolds stresses. According to RDT, the Reynolds stresses are determined not by the rate of strain, but by the total amount of mean strain experienced by the turbulence. In these circumstances the turbulence behaves not like a viscous fluid, but more like an elastic solid (Crow 1968): the turbulent viscosity hypothesis is qualitatively incorrect.

In the experiment depicted in Fig. 10.1, following the contraction there is a second straight section. Since there is no mean straining in this section, the turbulent-viscosity hypothesis inevitably predicts that the Reynolds-stress anisotropies are zero. However, the experimental data of Warhaft (1980) show instead that the anisotropies generated in the contraction decay quite slowly, on the turbulence timescale k/ε (see Fig. 10.2). These persisting anisotropies exist not because of the local mean strain rates (which are zero), but because of the prior history of straining to which the turbulence has been subjected.

Evidently, for this flow, both in the contraction section and in the downstream straight section, the intrinsic assumption of the turbulent-viscosity hypothesis is incorrect: the Reynolds-stress anisotropies are not determined by the local mean rates of strain.

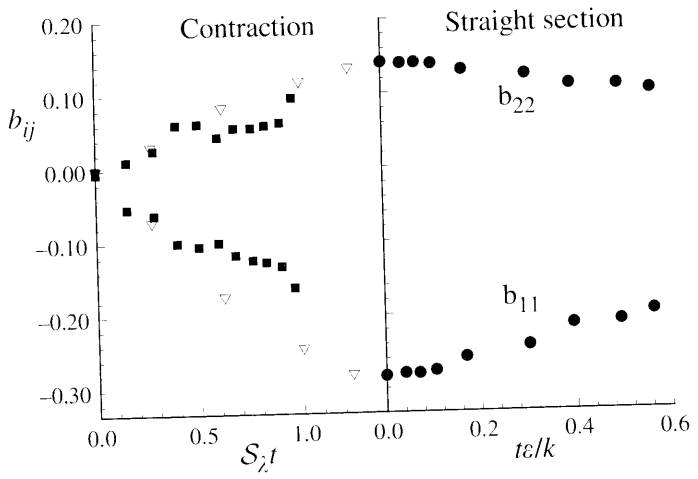

Fig. 10.2. Reynolds-stress anisotropies during and after axisymmetric straining. Contraction: experimental data of Tucker (1970), $\mathcal{S}_\lambda k/\varepsilon = 2.1$; △ DNS data of Lee and Reynolds (1985), $\mathcal{S}_\lambda k/\varepsilon = 55.7$; the flight time t from the beginning of the contraction is normalized by the mean strain rate $\mathcal{S}_\lambda$. Straight section: experimental data of Warhaft (1980); the flight time from the beginning of the straight section is normalized by the turbulence timescale there.

Comparison with kinetic theory

Simple kinetic theory for ideal gases (see, e.g., Vincenti and Kruger (1965) and Chapman and Cowling (1970)) yields the Newtonian viscous stress law (Eq. (10.6)), with the kinematic viscosity given by

$$\nu \approx \tfrac{1}{2}\bar{C}\lambda, \tag{10.7}$$

where $\bar{C}$ is the mean molecular speed, and λ is the mean free path. It is natural to seek to justify the turbulent-viscosity hypothesis through analogy with kinetic theory, and hence to give physical significance to u^* and ℓ^* by analogy to $\bar{C}$ and λ. However, a simple examination of the various timescales involved shows that such an analogy has no general validity.

In simple laminar shear flow (with shear rate $\partial U_1/\partial x_2 = \mathcal{S} = \mathcal{U}/\mathcal{L}$), the ratio of the molecular timescale $\lambda/\bar{C}$ and the shear timescale $\mathcal{S}^{-1}$ is

$$\frac{\lambda}{\bar{C}}\mathcal{S} = \frac{\lambda}{\mathcal{L}}\frac{\mathcal{U}}{\bar{C}} \sim \mathrm{KnMa}, \tag{10.8}$$

which is typically very small (e.g., 10^{-10}, see Exercise 10.1). The significance of the molecular timescale being relatively minute is that the statistical state of the molecular motion rapidly adjusts to the imposed straining. By contrast, for turbulent shear flows, the ratio of the turbulence timescale $\tau = k/\varepsilon$ to the mean shear timescale $\mathcal{S}^{-1}$ is not small: in the self-similar round jet $\mathcal{S}k/\varepsilon$ is

about 3 (Table 5.2 on page 131); in experiments on homogeneous turbulent shear flow it is typically 6 (Table 5.4 on page 157); and in turbulence subjected to rapid distortions it can be orders of magnitude larger. Consequently, as already observed, turbulence does not adjust rapidly to imposed mean straining, and so (in contrast to the case of molecular motion) there is no general basis for a local relationship between the stress and the rate of strain.

Simple shear flows

The example of rapid axisymmetric distortion and the timescale considerations given above show that, in general, the turbulent-viscosity hypothesis is incorrect. These general objections notwithstanding, there are important particular flows for which the hypothesis is more reasonable. In simple turbulent shear flows (e.g., the round jet, mixing layer, channel flow, and boundary layer) the turbulence characteristics and mean velocity gradients change relatively slowly (following the mean flow). As a consequence, the local mean velocity gradients characterize the history of the mean distortion to which the turbulence has been subjected; and the Reynolds-stress balance is dominated by local processes – production, dissipation, the pressure–rate-of-strain tensor – the non-local transport processes being small in comparison (see e.g., Figs. 7.35–7.38 on pages 316–317). In these circumstances, then, it is more reasonable to hypothesize that there is a relationship between the Reynolds stresses and the local mean velocity gradients.

An important observation is that in these particular flows (in which the turbulence characteristics change slowly following the mean flow), the production and dissipation of turbulent kinetic energy are approximately in balance, i.e., $\mathcal{P}/\varepsilon \approx 1$. By contrast, in the axisymmetric-contraction experiment (Fig. 10.1), in the contraction section $\mathcal{P}/\varepsilon$ is much greater than unity, whereas in the downstream straight section $\mathcal{P}/\varepsilon$ is zero: in both of these cases the turbulent-viscosity hypothesis is incorrect.

The gradient-diffusion hypothesis

Related to the turbulent-viscosity hypothesis is the gradient-diffusion hypothesis

$$\langle \boldsymbol{u}\phi' \rangle = -\Gamma_T \nabla \langle \phi \rangle, \tag{10.9}$$

according to which the scalar flux $\langle \boldsymbol{u}\phi' \rangle$ is aligned with the mean scalar gradient (see Section 4.4). Most of the observations made above apply equally to the gradient-diffusion hypothesis. In homogeneous shear flow it is found that the direction of the scalar flux is significantly different than that of the mean gradient (Tavoularis and Corrsin 1985). However, in simple two-dimensional

...ent shear flows (in the usual coordinate system) the scalar equation

$$\langle v\phi' \rangle = -\Gamma_T \frac{\partial \langle \phi \rangle}{\partial y}, \tag{10.10}$$

... used to define Γ_T, and thus no assumption is involved (for this ... ment). The turbulent Prandtl number σ_T can be used to relate ν_T and ... $\Gamma_T = \nu_T/\sigma_T$; and for simple shear flows, σ_T is of order unity (see, ... Fig. 5.34 on page 162).

... ν_T and Γ_T can be written as the product of a velocity scale and a ...scale (Eq. (10.3)). They can also be expressed as the product of the ... of a velocity scale and a timescale:

$$\Gamma_T = u^{*2} T^*. \tag{10.11}$$

...wn in Section 12.4, in ideal circumstances, Γ_T can be related to statis... the turbulence: u^* is the r.m.s. velocity u', and T^* is the Lagrangian ...al timescale T_L (see Eq. (12.158) on page 500).

EXERCISE

According to simple kinetic theory (see, e.g., Vincenti and Kruger (1965)) the kinematic viscosity of an ideal gas is

$$\nu \approx \tfrac{1}{2} \bar{C} \lambda, \tag{10.12}$$

and the mean molecular speed $\bar{C}$ is 1.35 times the speed of sound a. Show that the shear rate $\mathcal{S} = U/\mathcal{L}$ normalized by the molecular timescale $\lambda/\bar{C}$ is

$$\frac{\mathcal{S}\lambda}{\bar{C}} \approx 0.7 \mathrm{MaKn}, \tag{10.13}$$

where the Mach number and Knudsen number are defined by $\mathrm{Ma} \equiv U/a$ and $\mathrm{Kn} \equiv \lambda/\mathcal{L}$.

Use the relation $a^2 = \gamma p/\rho$ (with $\gamma = 1.4$) to show that the ratio of the viscous shear stress τ_{12} to the normal stress (pressure) is

$$\frac{\tau_{12}}{p} \approx 0.9 \mathrm{MaKn}. \tag{10.14}$$

Using the values $a = 332$ m s^{-1} and $\nu = 1.33 \times 10^{-5}$ m^2 s^{-1} (corresponding to air under atmospheric conditions) and $\mathcal{S} = 1$ s^{-1}, obtain the following estimates:

$$\lambda = 5.9 \times 10^{-8} \text{ m}, \quad \lambda/\bar{C} = 1.3 \times 10^{-10} \text{ s},$$
$$\frac{\mathcal{S}\lambda}{\bar{C}} = 1.3 \times 10^{-10}, \quad \frac{\tau_{12}}{p} = 1.7 \times 10^{-10}. \tag{10.15}$$

10.1.2 The specific assumption

We turn now to the *specific* assumption that the relationship between the Reynolds stresses and mean velocity gradients is that given by Eq. (10.1) (or, equivalently, Eq. (10.4) or (10.5)).

For simple shear flows, the single Reynolds stress of interest $\langle uv \rangle$ is related to the single significant mean velocity gradient $\partial \langle U \rangle / \partial y$ by Eq. (10.2). In essence, no assumption is involved, but rather the equation defines ν_T. Examples of profiles of ν_T thus obtained are given in Fig. 5.10 (on page 108) for the round jet, and in Fig. 7.30 (on page 307) for the boundary layer.

In general, the specific assumption in the turbulent-viscosity hypothesis is that the Reynolds-stress-anisotropy tensor a_{ij} is linearly related to the mean rate-of-strain tensor $\bar{S}_{ij}$ via the scalar turbulent viscosity, Eq. (10.5). Even for the simplest of flows, this is patently incorrect. In turbulent shear flow the normal strain rates are zero ($\bar{S}_{11} = \bar{S}_{22} = \bar{S}_{33} = 0$) and yet the normal Reynolds stresses are significantly different from each other (see Table 5.4 on page 157). An alternative perspective on the same observation is that the principal axes of a_{ij} are (by a significant amount) misaligned with those of $\bar{S}_{ij}$ (see Exercise 4.5 on page 90).

The reason that the simple linear stress law applies to the viscous stresses (Eq. (10.6)) but not to the Reynolds stresses can again be understood in terms of the timescale ratio, and in terms of the level of anisotropy. Compared with the molecular scales, the straining is very weak ($\mathcal{S}\lambda/\bar{C} \ll 1$), and consequently it produces a very small departure from isotropy: in simple laminar shear flow the ratio of anisotropic and isotropic molecular stresses is

$$\frac{\tau_{12}}{p} \approx \frac{\frac{1}{2}\bar{C}\lambda\mathcal{U}}{P\mathcal{L}} \sim \mathrm{KnMa}, \tag{10.16}$$

(see Exercise 10.1), which is typically very small. As a consequence, there is every reason to expect the anisotropic stresses to depend *linearly* on the velocity gradients. The Newtonian viscous stress law (Eq. (10.6)) is the most general possible *linear* relation consistent with the mathematical properties of the stress tensor. By contrast, in turbulent shear flow, the anisotropic-to-isotropic stress ratio $-\langle uv \rangle / (\frac{2}{3}k)$ is close to 0.5. In the turbulent case, then, the rate of straining is relatively large ($\mathcal{S}k/\varepsilon > 1$) and it leads to relatively large anisotropies. Consequently, there is no reason to suppose that the relationship is linear.

There are several classes of flows in which the mean velocity gradient tensor is more complex than that in simple shear flow, and in which the turbulent-viscosity hypothesis is known to fail significantly. Examples are strongly swirling flows (Weber, Visser, and Boysan 1990), flows with signif-

icant streamline curvature (Bradshaw 1973, Patel and Sotiropoulos 1997), and fully developed flow in ducts of non-circular cross-section (Melling and Whitelaw 1976, Bradshaw 1987).

In place of Eq. (10.5), a possible nonlinear turbulent viscosity hypothesis is

$$a_{ij} = -2\nu_{T1}\bar{S}_{ij} + \nu_{T2}(\bar{S}_{ik}\bar{\Omega}_{kj} - \bar{\Omega}_{ik}\bar{S}_{kj}) + \nu_{T3}(\bar{S}_{ik}\bar{S}_{kj} - \tfrac{1}{3}\bar{S}^2_{kk}\delta_{ij}), \quad (10.17)$$

where the coefficients ν_{T1}, ν_{T2} and ν_{T3} may depend on the mean-velocity-gradient invariants such as $\bar{S}^2_{kk}$ (as well as on turbulence quantities). Note that a dependence of a_{ij} on the mean rate of rotation $\bar{\Omega}_{ij}$ (e.g., through the term in ν_{T2}) is required so that the principal axes of a_{ij} are not aligned with those of $\bar{S}_{ij}$. Rational means of obtaining nonlinear turbulent viscosity laws have been developed, and are described in Section 11.9.

In summary: the *intrinsic* assumption of the turbulent-viscosity hypothesis – that a_{ij} is locally determined by $\partial\langle U_i\rangle/\partial x_j$ – has no general validity. However, for simple shear flows, in which the mean velocity gradients and turbulence characteristics evolve slowly (following the mean flow), the hypothesis is more reasonable. In such flows $\mathcal{P}/\varepsilon$ is close to unity, which is indicative of an approximate local balance in the Reynolds-stress equations between production by the mean shear and the other local processes – redistribution and dissipation.

10.2 Algebraic models

The algebraic models that have been introduced in previous chapters are the *uniform turbulent viscosity* and the *mixing-length model*. These models are now appraised relative to the criteria described in Chapter 8.

10.2.1 Uniform turbulent viscosity

In applications to a planar two-dimensional free shear flow, the uniform-turbulent-viscosity model can be written

$$\nu_T(x, y) = \frac{U_0(x)\delta(x)}{R_T}, \quad (10.18)$$

where $U_0(x)$ and $\delta(x)$ are the characteristic velocity scale and lengthscale of the mean flow, and R_T – which has the interpretation of a turbulent Reynolds number – is a flow-dependent constant. Thus the turbulent viscosity is taken to be constant across the flow (in the y direction), but it varies in the mean-flow direction.

The range of applicability of this model is extremely limited. In order to

Table 10.1. *Measured spreading rates S and corresponding values of the turbulent Reynolds number* R_T *for self-similar free shear flows*

Flow	Spreading rate S	Turbulent Reynolds number, R_T	Equation relating S to R_T
Round jet	0.094	35	5.84
Plane jet	0.10	31	5.200
Mixing layer	0.06–0.11	60–110	5.225
Plane wake	0.073–0.103	13–19	5.241
Axisymmetric wake	0.064–0.8	2–22	5.260

apply the model, it is necessary to define unambiguously the direction of flow, x; the characteristic flow width $\delta(x)$; and the characteristic velocity $U_0(x)$. This is possible only for the simplest of flows.

For the simple free shear flows to which it is applicable, the model is incomplete, in that R_T has to be specified. The appropriate value depends both upon the nature of the flow and on the definitions chosen for $\delta(x)$ and $U_0(x)$. In Chapter 5, it is shown that, for each self-similar free shear flow, there is an inverse relation between the rate of spreading S and the turbulent Reynolds number R_T. Table 10.1 summarizes the measured spreading rates and the corresponding values of R_T. (For each flow, the definitions of S, δ, and U_0 are given in Chapter 5.)

In self-similar free shear flows, the empirically determined turbulent viscosity is fairly uniform over the bulk of the flow, but it decreases to zero as the free stream is approached (see, e.g., Fig. 5.10 on page 108). Correspondingly, the mean velocity profile predicted by the uniform viscosity model agrees well with experimental data except at the edge of the flow (e.g., Fig. 5.15 on page 119).

In principle, the uniform-turbulent-viscosity model could be applied to simple wall-bounded flows. However, since the turbulent viscosity in fact varies significantly across the flow (see Fig. 7.30 on page 307), the resulting predicted mean velocity profile would be, for most purposes, uselessly inaccurate.

In summary, the uniform-turbulent-viscosity model provides a useful basic description of the mean velocity profiles in self-similar free shear flows. However, it is an incomplete model with a very limited range of applicability.

10.2.2 The mixing-length model

In application to two-dimensional boundary-layer flows, the mixing length $\ell_m(x, y)$ is specified as a function of position, and then the turbulent viscosity

is obtained as

$$\nu_T = \ell_m^2 \left| \frac{\partial \langle U \rangle}{\partial y} \right|. \tag{10.19}$$

As shown in Section 7.1.7, in the log-law region, the appropriate specification of the mixing length is $\ell_m = \kappa y$, and then the turbulent viscosity is $\nu_T = u_\tau \kappa y$.

Several generalizations of Eq. (10.19) have been proposed in order to allow the application of the mixing-length hypothesis to all flows. On the basis of the mean rate of strain $\bar{S}_{ij}$ Smagorinsky (1963) proposed

$$\nu_T = \ell_m^2 (2\bar{S}_{ij}\bar{S}_{ij})^{1/2} = \ell_m^2 \mathcal{S}, \tag{10.20}$$

whereas, on the basis of the mean rate of rotation $\bar{\Omega}_{ij}$, Baldwin and Lomax (1978) proposed

$$\nu_T = \ell_m^2 (2\bar{\Omega}_{ij}\bar{\Omega}_{ij})^{1/2} = \ell_m^2 \Omega. \tag{10.21}$$

(Both of these formulae reduce to Eq. (10.19) in the case that $\partial \langle U_1 \rangle / \partial x_2$ is the only non-zero mean velocity gradient.)

In its generalized form, the mixing-length model is applicable to all turbulent flows, and it is arguably the simplest turbulence model. Its major drawback, however, is its incompleteness: the mixing length $\ell_m(\boldsymbol{x})$ has to be specified, and the appropriate specification is inevitably dependent on the geometry of the flow. For a complex flow that has not been studied before, the specification of $\ell_m(\boldsymbol{x})$ requires a large measure of guesswork, and consequently one should have little confidence in the accuracy of the resulting calculated mean velocity field. On the other hand, there are classes of technologically important flows that have been studied extensively, so that the appropriate specifications of $\ell_m(\boldsymbol{x})$ are well established. The prime example is boundary-layer flows in aeronautical applications. The Cebeci–Smith model (Smith and Cebeci 1967) and the Baldwin–Lomax model (Baldwin and Lomax 1978) provide mixing-length specifications that yield quite accurate calculations of attached boundary layers. Details of these models and their performance are provided by Wilcox (1993).

As illustrated in the following exercise, the mixing-length model can also be applied to free shear flows. The predicted mean velocity profile agrees well with experimental data (see, e.g., Schlichting (1979)). An interesting (though non-physical) feature of the solution is that the mixing layer has a definite edge at which the mean velocity goes to the free-stream velocity with zero slope but non-zero curvature.

EXERCISE

10.2 Consider the self-similar temporal mixing layer in which the mean lateral velocity $\langle V \rangle$ is zero, and the axial velocity $\langle U \rangle$ depends on y and t only. The velocity difference is U_s, so that the boundary conditions are $\langle U \rangle = \pm\frac{1}{2}U_s$ at $y = \pm\infty$. The thickness of the layer $\delta(t)$ is defined (as in Fig. 5.21 on page 140) such that $\langle U \rangle = \pm\frac{2}{5}U_s$ at $y = \pm\frac{1}{2}\delta$.

The mixing-length model is applied to this flow, with the mixing length being uniform across the flow and proportional to the flow's width, i.e., $\ell_m = \alpha\delta$, where α is a specified constant.

Starting from the Reynolds equations

$$\frac{\partial\langle U \rangle}{\partial t} = -\frac{\partial\langle uv \rangle}{\partial y}, \tag{10.22}$$

show that the mixing-length hypothesis implies that

$$\frac{\partial\langle U \rangle}{\partial t} = 2\alpha^2\delta^2 \frac{\partial\langle U \rangle}{\partial y}\frac{\partial^2\langle U \rangle}{\partial y^2}. \tag{10.23}$$

Show that this equation admits a self-similar solution of the form $\langle U \rangle = U_s f(\xi)$, where $\xi = y/\delta$; and that $f(\xi)$ satisfies the ordinary differential equation

$$-S\xi f' = 2\alpha^2 f' f'', \tag{10.24}$$

where $S \equiv U_s^{-1}\,\mathrm{d}\delta/\mathrm{d}t$ is the spreading rate.

Show that Eq. (10.24) admits two different solutions (denoted by f_1 and f_2):

$$f_1 = -\frac{S}{12\alpha^2}\xi^3 + A\xi + B, \tag{10.25}$$

$$f_2 = C, \tag{10.26}$$

where A, B, and C are arbitrary constants.

The appropriate solution for f is made up of three parts. For $|\xi|$ greater than a particular value ξ^*, f is constant (i.e., f_2):

$$f = \begin{cases} -\frac{1}{2} & \text{for } \xi < -\xi^*, \\ \frac{1}{2} & \text{for } \xi > \xi^*. \end{cases} \tag{10.27}$$

Show that the appropriate solution for $-\xi^* < \xi < \xi^*$ satisfying $f'(\pm\xi^*) = 0$ is

$$f = \frac{3}{4}\frac{\xi}{\xi^*} - \frac{1}{4}\left(\frac{\xi}{\xi^*}\right)^3. \tag{10.28}$$

Show that the spreading rate is related to the mixing-length constant by

$$S = 3\alpha^2/\xi^{*3}, \tag{10.29}$$

and use the definition of δ (i.e., $f\left(\frac{1}{2}\right) = \frac{2}{5}$) to obtain

$$\xi^* \approx 0.8450. \tag{10.30}$$

How does ν_T vary across the flow?

10.3 Turbulent-kinetic-energy models

With the turbulent viscosity written as

$$\nu_T = \ell^* u^*, \tag{10.31}$$

in the mixing-length model the lengthscale is $\ell^* = \ell_m$ and the velocity scale is (in simple shear flow)

$$u^* = \ell_m \left| \frac{\partial \langle U \rangle}{\partial y} \right|. \tag{10.32}$$

The implication is that the velocity scale is locally determined by the mean velocity gradient; and, in particular, u^* is zero where $\partial\langle U\rangle/\partial y$ is zero. In fact, contrary to this implication, there are several circumstances in which the velocity gradient is zero and yet the turbulent velocity scale is non-zero. One example is decaying grid turbulence; another is the centerline of the round jet, where direct measurement shows ν_T to be far from zero (see Fig. 5.10 on page 108).

Independently, Kolmogorov (1942) and Prandtl (1945) suggested that it is better to base the velocity scale on the turbulent kinetic energy, i.e.,

$$u^* = ck^{1/2}, \tag{10.33}$$

where c is a constant. If the lengthscale is again taken to be the mixing length, then the turbulent viscosity becomes

$$\nu_T = ck^{1/2}\ell_m. \tag{10.34}$$

As shown in Exercise 10.3, the value of the constant $c \approx 0.55$ yields the correct behavior in the log-law region.

In order for Eq. (10.34) to be used, the value of $k(\boldsymbol{x}, t)$ must be known or estimated. Kolmogorov and Prandtl suggested achieving this by solving a model transport equation for k. This is called a *one-equation model*, because a

model transport equation is solved for just one turbulence quantity, namely, k.

Before discussing the model transport equation for k, it is helpful to itemize all the components of the model:

(i) the mixing length $\ell_m(\boldsymbol{x}, t)$ is specified;
(ii) a model transport equation is solved for $k(\boldsymbol{x}, t)$;
(iii) the turbulent viscosity is defined by $\nu_T = ck^{1/2}\ell_m$;
(iv) the Reynolds stresses are obtained from the turbulent-viscosity hypothesis, Eq. (10.1); and
(v) the Reynolds equations are solved for $\langle \boldsymbol{U}(\boldsymbol{x}, t)\rangle$ and $\langle p(\boldsymbol{x}, t)\rangle$.

Thus, from the specification of ℓ_m and from the solutions to the exact and model equations, the following fields are determined: $\langle \boldsymbol{U}\rangle$, $\langle p\rangle$, ℓ_m, k, ν_T, and $\langle u_i u_j\rangle$. These are referred to as 'knowns.'

We now consider the model transport equation for k. The exact equation (Eq. (5.132)) is

$$\frac{\bar{\mathrm{D}}k}{\bar{\mathrm{D}}t} \equiv \frac{\partial k}{\partial t} + \langle \boldsymbol{U}\rangle \cdot \nabla k = -\nabla \cdot \boldsymbol{T}' + \mathcal{P} - \varepsilon, \tag{10.35}$$

where the flux $\boldsymbol{T}'$ (Eq. (5.140)) is

$$T_i' = \tfrac{1}{2}\langle u_i u_j u_j\rangle + \langle u_i p'\rangle/\rho - 2\nu\langle u_j s_{ij}\rangle. \tag{10.36}$$

In Eq. (10.35), any term that is completely determined by the 'knowns' is said to be 'in closed form.' Specifically, $\bar{\mathrm{D}}k/\bar{\mathrm{D}}t$ and $\mathcal{P}$ are in closed form. Conversely, the remaining terms (ε and $\nabla \cdot \boldsymbol{T}'$) are 'unknown' and, in order to obtain a closed set of model equations, these terms must be modelled. That is, 'closure approximations' that model the unknowns in terms of the knowns are required.

As discussed extensively in Chapter 6, at high Reynolds number the dissipation rate ε scales as u_0^3/ℓ_0, where u_0 and ℓ_0 are the velocity scale and lengthscale of the energy-containing motions. Consequently, it is reasonable to model ε as

$$\varepsilon = C_D k^{3/2}/\ell_m, \tag{10.37}$$

where C_D is a model constant. Indeed, an examination of the log-law region (Exercise 10.3) yields this relation with $C_D = c^3$.

Modelling assumptions such as Eq. (10.37) deserve close scrutiny. Equations (10.34) and (10.37) can be combined to eliminate ℓ_m to yield

$$\nu_T = cC_D k^2/\varepsilon, \tag{10.38}$$

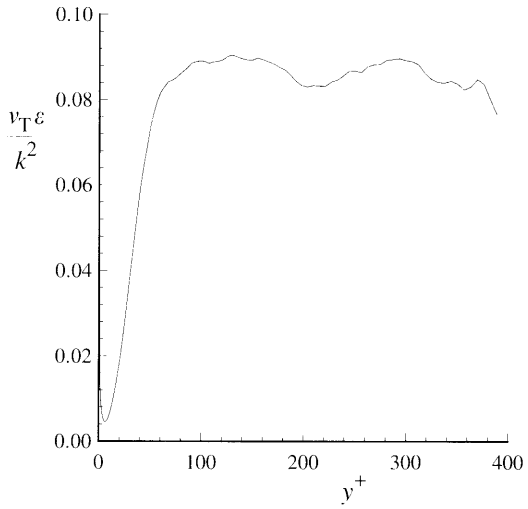

Fig. 10.3. The profile of $\nu_T \varepsilon / k^2$ (see Eq. (10.39)) from DNS of channel flow at $Re = 13,750$ (Kim *et al.* 1987).

or equivalently,

$$\frac{\nu_T \varepsilon}{k^2} = c C_D. \tag{10.39}$$

For simple shear flows, k, ε, and $\nu_T = -\langle uv \rangle / (\partial \langle U \rangle / \partial y)$ can be measured, so that this modelling assumption can be tested directly. Figure 10.3 shows the left-hand side of Eq. (10.39) extracted from DNS data of fully developed turbulent channel flow. It may be seen that (except close to the wall, $y^+ < 50$) this quantity is indeed approximately constant, with a value around 0.09. Figure 10.4 shows the same quantity for the temporal-mixing layer: except near the edges, the value is everywhere close to 0.08.

The remaining unknown in the turbulent-kinetic-energy equation is the energy flux $\boldsymbol{T}'$ (Eq. (10.36)). This is modelled with a gradient-diffusion hypothesis as

$$\boldsymbol{T}' = -\frac{\nu_T}{\sigma_k} \nabla k, \tag{10.40}$$

where the 'turbulent Prandtl number' for kinetic energy[1] is generally taken to be $\sigma_k = 1.0$. Physically, Eq. (10.40) asserts that (due to velocity and pressure fluctuations) there is a flux of k down the gradient of k. Mathematically, the term ensures that the resulting model transport equation for k yields smooth solutions, and that a boundary condition can be imposed on k everywhere on the boundary of the solution domain.

[1] The symbol σ_k is standard notation. Note, however, that σ_k is a scalar, and that 'k' is not a suffix in the sense of Cartesian-tensor suffix notation.

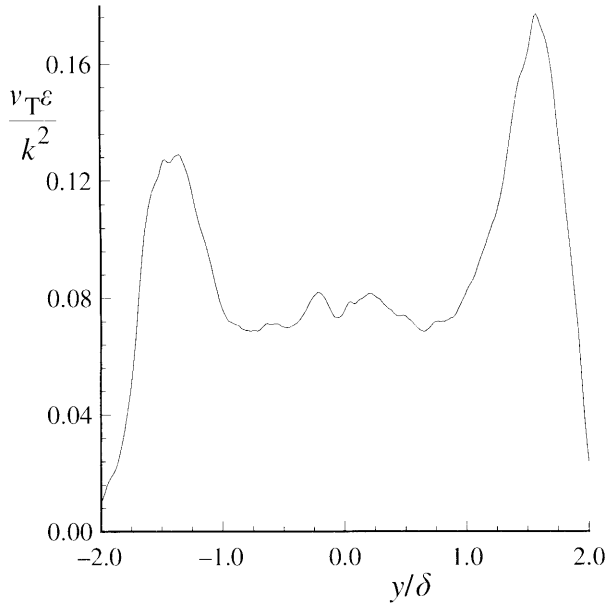

Fig. 10.4. The profile of $\nu_T \varepsilon / k^2$ (see Eq. (10.39)) from DNS of the temporal mixing layer. (From data of Rogers and Moser (1994)).)

In summary, the one-equation model based on k consists of the model transport equation

$$\frac{\bar{\mathrm{D}}k}{\bar{\mathrm{D}}t} = \nabla \cdot \left(\frac{\nu_T}{\sigma_k} \nabla k \right) + \mathcal{P} - \varepsilon, \tag{10.41}$$

with $\nu_T = c k^{1/2} \ell_m$ and $\varepsilon = C_D k^{3/2} / \ell_m$, together with the turbulent-viscosity hypothesis (Eq. (10.1)) and the specification of ℓ_m.

A comparison of model predictions with experimental data (Wilcox 1993) shows that this one-equation model has a modest advantage in accuracy over mixing-length models. However, the major drawback of incompleteness remains: the length scale $\ell_m(\boldsymbol{x})$ must be specified.

EXERCISES

10.3 Consider the log-law region of a wall-bounded flow. Use the log-law and the specification $\ell_m = \kappa y$ to show that the appropriate value of the constant c (in the relation $\nu_T = c k^{1/2} \ell_m$) is

$$c = |\langle uv \rangle / k|^{1/2} \approx 0.55. \tag{10.42}$$

Use the relation $\mathcal{P} = \varepsilon$ to show that

$$\varepsilon = c^3 k^{3/2} / \ell_m, \tag{10.43}$$

and hence

$$\nu_T = c^4 k^2/\varepsilon. \tag{10.44}$$

10.4 For the one-equation model applied to simple shear flow, express the production $\mathcal{P}$ in terms of k, ℓ_m and $\partial\langle U\rangle/\partial y$. Hence (taking $C_D = c^3$ in Eq. (10.37)) show that the velocity scales u^* in the one-equation model and in the mixing-length model are related by

$$ck^{1/2} = \ell_m \left|\frac{\partial\langle U\rangle}{\partial y}\right| \left(\frac{\mathcal{P}}{\varepsilon}\right)^{-1/2} \tag{10.45}$$

Show that the corresponding relation for a general flow is

$$ck^{1/2} = \ell_m \mathcal{S} \left(\frac{\mathcal{P}}{\varepsilon}\right)^{-1/2} \tag{10.46}$$

(cf. Eq. (10.20)).

10.4 The k–ε model

10.4.1 An overview

The k–ε model belongs to the class of *two-equation models*, in which model transport equations are solved for two turbulence quantities – i.e., k and ε in the k–ε model. From these two quantities can be formed a lengthscale ($L = k^{3/2}/\varepsilon$), a timescale ($\tau = k/\varepsilon$), a quantity of dimension ν_T (k^2/ε), etc. As a consequence, two-equation models can be *complete* – flow-dependent specifications such as $\ell_m(\boldsymbol{x})$ are not required.

The k–ε model is the most widely used complete turbulence model, and it is incorporated in most commercial CFD codes. As is the case with all turbulence models, both the concepts and the details evolved over time; but Jones and Launder (1972) are appropriately credited with developing the 'standard' k–ε model, with Launder and Sharma (1974) providing improved values of the model constants. Significant earlier contributions are due to Davidov (1961), Harlow and Nakayama (1968), Hanjalić (1970), and others cited by Launder and Spalding (1972).

In addition to the turbulent viscosity hypothesis, the k–ε model consists of

(i) the model transport equation for k (which is the same as that in the one-equation model, Eq. (10.41));
(ii) the model transport equation for ε (which is described below); and

(iii) the specification of the turbulent viscosity as

$$\nu_T = C_\mu k^2/\varepsilon, \tag{10.47}$$

where $C_\mu = 0.09$ is one of five model constants.

If it is supposed that ν_T depends only on the turbulence quantities k and ε (independent of $\partial\langle U_i\rangle/\partial x_j$ etc.), then Eq. (10.47) is inevitable. The one-equation model implies the similar relation $\nu_T = c^4k^2/\varepsilon$ (see Exercise 10.3), so the model constants are related by $c = C_\mu^{1/4}$.

In simple turbulent shear flow, the k–ε model yields

$$\frac{|\langle uv\rangle|}{k} = \left(C_\mu \frac{\mathcal{P}}{\varepsilon}\right)^{1/2}, \tag{10.48}$$

(see Exercise 10.5) so that the specification $C_\mu = 0.09 = (0.3)^2$ stems from the empirical observation $|\langle uv\rangle|/k \approx 0.3$ in regions where $\mathcal{P}/\varepsilon$ is close to unity.

The quantity $\nu_T\varepsilon/k^2$ plotted in Figs. 10.3 and 10.4 is a 'measurement' of C_μ for channel flow and for the temporal mixing layer. As may be seen, $\nu_T\varepsilon/k^2$ is close to the value 0.09 everywhere except near the boundaries of the flows.

EXERCISE

10.5 Consider the k–ε model applied to a simple turbulent shear flow with $S = \partial\langle U\rangle/\partial y$ being the only non-zero mean velocity gradient. Obtain the relations

$$\frac{|\langle uv\rangle|}{k} = C_\mu \frac{Sk}{\varepsilon}, \tag{10.49}$$

$$\frac{\mathcal{P}}{\varepsilon} = C_\mu \left(\frac{Sk}{\varepsilon}\right)^2, \tag{10.50}$$

and hence verify Eq. (10.48).

Show that $\langle uv\rangle$ satisfies the Cauchy–Schwartz inequality (Eq. (3.100)) if, and only if, C_μ satisfies

$$C_\mu \le \frac{2/3}{Sk/\varepsilon}, \tag{10.51}$$

or, equivalently,

$$C_\mu \le \frac{4/9}{\mathcal{P}/\varepsilon}. \tag{10.52}$$

Show that Eq. (10.50) also holds for a general flow.

10.4.2 The model equation for ε

Quite different approaches are taken in developing the model transport equations for k and ε. The k equation amounts to the exact equation (Eq. (10.35)) with the turbulent flux $\boldsymbol{T}'$ modelled as gradient diffusion (Eq. (10.40)). The three other terms – $\bar{\mathrm{D}}k/\bar{\mathrm{D}}t$, $\mathcal{P}$, and ε – are in closed form (given the turbulent-viscosity hypothesis).

The exact equation for ε can also be derived, but it is not a useful starting point for a model equation. This is because (as discussed in Chapter 6) ε is best viewed as the energy-flow rate in the cascade, and it is determined by the large-scale motions, independent of the viscosity (at high Reynolds number). By contrast, the exact equation for ε pertains to processes in the dissipative range. Consequently, rather than being based on the exact equation, the standard model equation for ε is best viewed as being entirely empirical: it is

$$\frac{\bar{\mathrm{D}}\varepsilon}{\bar{\mathrm{D}}t} = \nabla \cdot \left(\frac{\nu_{\mathrm{T}}}{\sigma_\varepsilon} \nabla \varepsilon \right) + C_{\varepsilon 1} \frac{\mathcal{P}\varepsilon}{k} - C_{\varepsilon 2} \frac{\varepsilon^2}{k}. \tag{10.53}$$

The standard values of all the model constants due to Launder and Sharma (1974) are

$$C_\mu = 0.09,\ C_{\varepsilon 1} = 1.44,\ C_{\varepsilon 2} = 1.92,\ \sigma_k = 1.0,\ \sigma_\varepsilon = 1.3. \tag{10.54}$$

An understanding of the ε equation can be gained by studying its behaviors in various flows. We first examine homogeneous turbulence, for which the k and ε equations become

$$\frac{\mathrm{d}k}{\mathrm{d}t} = \mathcal{P} - \varepsilon, \tag{10.55}$$

$$\frac{\mathrm{d}\varepsilon}{\mathrm{d}t} = C_{\varepsilon 1} \frac{\mathcal{P}\varepsilon}{k} - C_{\varepsilon 2} \frac{\varepsilon^2}{k}. \tag{10.56}$$

Decaying turbulence

In the absence of mean velocity gradients, the production is zero, and the turbulence decays. The equations then have the solutions

$$k(t) = k_0 \left(\frac{t}{t_0} \right)^{-n}, \quad \varepsilon(t) = \varepsilon_0 \left(\frac{t}{t_0} \right)^{-(n+1)}, \tag{10.57}$$

where k and ε have the values k_0 and ε_0 at the reference time

$$t_0 = n \frac{k_0}{\varepsilon_0}, \tag{10.58}$$

and the decay exponent n is

$$n = \frac{1}{C_{\varepsilon 2} - 1}. \tag{10.59}$$

This power-law decay is precisely that observed in grid turbulence (see Section 5.4.6, Eqs. (5.274) and (5.277)), and so the behavior of the ε equation is correct for this flow.

The experimental values reported for the decay exponent n are generally in the range 1.15–1.45, and Mohamed and LaRue (1990) suggest that most of the data are consistent with $n = 1.3$. Equation (10.59) can be rearranged to give $C_{\varepsilon 2}$ in terms of n :

$$C_{\varepsilon 2} = \frac{n+1}{n}, \tag{10.60}$$

and the values of $C_{\varepsilon 2}$ corresponding to $n = 1.15$, 1.3, and 1.45, are 1.87, 1.77, and 1.69. It may be seen, then, that the standard value ($C_{\varepsilon 2} = 1.92$) lies somewhat outside of the experimentally observed range. The reason for this is discussed below.

EXERCISES

10.6 Consider the k–ε model applied to decaying turbulence. Let $s(t)$ be the normalized time defined by

$$s(t) = \int_{t_0}^{t} \frac{\varepsilon(t')}{k(t')}\, \mathrm{d}t'.$$

(a) Obtain an explicit expression for $s(t)$.
(b) Derive and solve evolution equations in s for k and ε (i.e., $\mathrm{d}k/\mathrm{d}s = \ldots$).
(c) Grid turbulence is examined between $x/M = 40$ and $x/M = 200$. To what interval in normalized time does this correspond?

10.7 Show that the k–ε model gives the correct behavior for the final period of decay (see Exercise 6.11 on page 205), if $C_{\varepsilon 2}$ is modified to $C_{\varepsilon 2} = \frac{7}{5}$.

Homogeneous shear flow

As observed in Section 5.4.5, in homogeneous turbulent shear flow, the principal experimental observations are that the Reynolds stresses become self-similar, and that the non-dimensional parameters $\mathcal{S}k/\varepsilon$ and $\mathcal{P}/\varepsilon$ become constant: $\mathcal{S}k/\varepsilon \approx 6$ and $\mathcal{P}/\varepsilon \approx 1.7$. Since the imposed mean shear rate $\mathcal{S}$ is

constant, the constancy of $\mathcal{S}k/\varepsilon$ implies that the turbulence timescale $\tau \equiv k/\varepsilon$ is also fixed. From the k and ε equations (Eqs. (10.55) and (10.56)) we obtain

$$\frac{\mathrm{d}}{\mathrm{d}t}\left(\frac{k}{\varepsilon}\right) = \frac{\mathrm{d}\tau}{\mathrm{d}t} = (C_{\varepsilon 2} - 1) - (C_{\varepsilon 1} - 1)\left(\frac{\mathcal{P}}{\varepsilon}\right). \tag{10.61}$$

Evidently the model predicts that τ does not change with time for the particular value of $\mathcal{P}/\varepsilon$,

$$\left(\frac{\mathcal{P}}{\varepsilon}\right)^* \equiv \frac{C_{\varepsilon 2} - 1}{C_{\varepsilon 1} - 1} \approx 2.1, \tag{10.62}$$

a considerably higher value than is observed in experiments and DNS.

Interpretation of the ε equation

We now offer an interpretation of the ε equation based on the relationship between the turbulence frequency $\omega \equiv \varepsilon/k$ and the characteristic mean strain rate $\mathcal{S}$.

An overly simple model is

$$\omega = \frac{\mathcal{S}}{\beta}, \tag{10.63}$$

where β is a constant; equal to 3, say. This model then predicts that $\mathcal{S}k/\varepsilon = \mathcal{S}/\omega$ is equal to the constant value $\beta = 3$ in all flows. In several shear flows this value of $\mathcal{S}k/\varepsilon$ is indeed measured (see Tables 5.2, 5.4, and 7.2 on pages 131, 157 and 283). However, for other flows the model is wrong: in grid turbulence ($\mathcal{S} = 0$) ω is not zero; and in homogeneous shear flow $\mathcal{S}k/\varepsilon$ is approximately 6.

Instead of setting ω *equal* to $\mathcal{S}/\beta$, consider instead a model that makes ω *relax* toward $\mathcal{S}/\beta$. Or (as a contrivance to produce the required result) consider the model that makes ω^2 relax toward $(\mathcal{S}/\beta)^2$. When it is applied to homogeneous turbulence, this model is described by the equation

$$\frac{\mathrm{d}\omega^2}{\mathrm{d}t} = -\alpha\omega\left(\omega^2 - \frac{\mathcal{S}^2}{\beta^2}\right), \tag{10.64}$$

where α is a constant and $\alpha\omega$ is the relaxation rate. It is a matter of algebra (see Exercise 10.8) to show that this equation is exactly equivalent to the ε equation (Eq. (10.56)) if the constants are specified as

$$\alpha = 2(C_{\varepsilon 2} - 1) \approx 1.84, \tag{10.65}$$

$$\beta = \left(\frac{C_{\varepsilon 2} - 1}{C_\mu[C_{\varepsilon 1} - 1]}\right)^{1/2} \approx 4.27. \tag{10.66}$$

Thus the ε equation can be interpreted through Eq. (10.64): at the rate $\alpha\omega$, the turbulence frequency (squared) relaxes toward $\mathcal{S}/\beta$ (squared).

EXERCISE

10.8 For homogeneous turbulence, from the model equations for k (Eq. (10.55)) and for ω^2 (Eq. (10.64)), show that the corresponding model equation for ε is

$$\frac{\mathrm{d}\varepsilon}{\mathrm{d}t} = \frac{\mathcal{P}\varepsilon}{k} + \frac{\alpha k \mathcal{S}^2}{2\beta^2} - (1 + \tfrac{1}{2}\alpha)\frac{\varepsilon^2}{k}. \tag{10.67}$$

By using Eq. (10.50) to eliminate $\mathcal{S}$, re-express the equation as

$$\frac{\mathrm{d}\varepsilon}{\mathrm{d}t} = \left(1 + \frac{\alpha}{2\beta^2 C_\mu}\right)\frac{\mathcal{P}\varepsilon}{k} - (1 + \tfrac{1}{2}\alpha)\frac{\varepsilon^2}{k}. \tag{10.68}$$

By comparing this result with the standard ε equation (Eq. (10.56)), verify the relationships between α and β, and $C_{\varepsilon 1}$ and $C_{\varepsilon 2}$ (Eqs. (10.65) and (10.66)).

The behavior in the log-law region

For inhomogeneous flows, the diffusion term in the ε equation (i.e., $\nabla \cdot [(\nu_\mathrm{T}/\sigma_\varepsilon)\nabla\varepsilon]$) has the same benefits as the analogous term in the k equation: it ensures that we obtain smooth solutions and it allows the specification of a boundary condition on ε everywhere on the boundary. As is now illustrated, the diffusion term plays an important role in near-wall flows.

Consider high-Reynolds-number, fully developed channel flow. The quantities of interest ($\langle U \rangle$, k, and ε) depend only on y, so that the k–ε equations reduce to

$$0 = \frac{\mathrm{d}}{\mathrm{d}y}\left(\frac{\nu_\mathrm{T}}{\sigma_k}\frac{\mathrm{d}k}{\mathrm{d}y}\right) + \mathcal{P} - \varepsilon, \tag{10.69}$$

$$0 = \frac{\mathrm{d}}{\mathrm{d}y}\left(\frac{\nu_\mathrm{T}}{\sigma_\varepsilon}\frac{\mathrm{d}\varepsilon}{\mathrm{d}y}\right) + C_{\varepsilon 1}\frac{\mathcal{P}\varepsilon}{k} - C_{\varepsilon 2}\frac{\varepsilon^2}{k}. \tag{10.70}$$

We now focus on the log-law region. Production and dissipation balance, both being equal to $u_\tau^3/(\kappa y)$. Hence in the k equation the diffusion term is zero, which implies that k is uniform, which is approximately correct. In the ε equation, the equality of $\mathcal{P}$ and ε leads to a net sink (equal to $-(C_{\varepsilon 2} - C_{\varepsilon 1})\varepsilon^2/k$) that varies as y^{-2}. This is balanced by the diffusion of ε away from the wall.

It is shown in Exercise 10.9 that the ε equation (Eq. (10.70)) is satisfied by

$$\varepsilon = \frac{C_\mu^{3/4} k^{3/2}}{\kappa y}, \tag{10.71}$$

and that the constants are related by

$$\kappa^2 = \sigma_\varepsilon C_\mu^{1/2} (C_{\varepsilon 2} - C_{\varepsilon 1}). \tag{10.72}$$

Equation (10.72) yields a value of the von Kármán constant implied by the k–ε model ($\kappa \approx 0.43$): or, alternatively, it can be used to adjust a model constant (e.g., σ_ε) to produce a particular value of κ.

EXERCISE

10.9 Consider the log-law region of a wall-bounded turbulent flow. Show that the turbulent viscosity hypothesis with $\nu_T = C_\mu k^2/\varepsilon$ and the log-law imply that

$$\varepsilon = \frac{C_\mu k^2}{u_\tau \kappa y}. \tag{10.73}$$

Given $\mathcal{P} = \varepsilon$, from the expression for $\mathcal{P}$ obtain the result

$$\varepsilon = \frac{C_\mu^{1/2} k u_\tau}{\kappa y}. \tag{10.74}$$

Hence verify Eq. (10.71) and compare it with Eq. (10.43). Substitute Eq. (10.71) for ε into the ε equation (Eq. (10.70), with k independent of y) to obtain Eq. (10.72). Verify that these equations yield the variation of the lengthscale

$$L \equiv \frac{k^{3/2}}{\varepsilon} = C_\mu^{3/4} \kappa y. \tag{10.75}$$

The behavior at the free-stream edge

As described in Section 5.5.2, there is an intermittent region between a turbulent flow and an irrotational, non-turbulent free stream or quiescent surroundings. In the non-turbulent fluid ($y \to \infty$), both k and ε are zero.

The k–ε model does not account for intermittency, and it yields solutions in which there is a sharp edge between the turbulent and non-turbulent regions (Cazalbou, Spalart, and Bradshaw 1994). For a statistically two-dimensional boundary layer or free shear flow, let $y_e(x)$ denote the location of the edge. Then, for $y > y_e(x)$, k and ε are zero, and the mean flow is irrotational. Just inside of the turbulent region, k, ε, and $\partial\langle U\rangle/\partial y$ vary as positive powers of the distance to the edge $y_e(x) - y$.

Because of entrainment, there is a mean flow through the edge from the non-turbulent side. The edge therefore corresponds to a turbulent front that propagates (relative to the fluid) by turbulent diffusion. The solutions to the k–ε model equations for such a propagating front are developed in Exercise 10.10.

EXERCISES

10.10 Consider a statistically stationary one-dimensional flow without turbulence production in which the k–ε equations reduce to

$$U_0 \frac{\mathrm{d}k}{\mathrm{d}x} = \frac{\mathrm{d}}{\mathrm{d}x}\left(\frac{\nu_\mathrm{T}}{\sigma_k}\frac{\mathrm{d}k}{\mathrm{d}x}\right) - \varepsilon, \tag{10.76}$$

$$U_0 \frac{\mathrm{d}\varepsilon}{\mathrm{d}x} = \frac{\mathrm{d}}{\mathrm{d}x}\left(\frac{\nu_\mathrm{T}}{\sigma_\varepsilon}\frac{\mathrm{d}\varepsilon}{\mathrm{d}x}\right) - C_{\varepsilon 2}\frac{\varepsilon^2}{k}, \tag{10.77}$$

where U_0 is the uniform mean velocity, which is positive. These equations admit a weak solution (with $k = 0$ and $\varepsilon = 0$ for $x \leq 0$ and $k > 0$ and $\varepsilon > 0$ for $x > 0$) corresponding to a front between turbulent flow ($x > 0$) and non-turbulent flow ($x \leq 0$). For small positive x the solutions are

$$k = k_0\left(\frac{x}{\delta_0}\right)^p, \tag{10.78}$$

$$\varepsilon = \varepsilon_0\left(\frac{x}{\delta_0}\right)^q, \tag{10.79}$$

where p, q, k_0, ε_0, and δ_0 are positive constants, with $\delta_0 \equiv k_0^{3/2}/\varepsilon_0$. By substituting Eqs. (10.78) and (10.79) into Eqs. (10.76) and (10.77), obtain the results

$$q = 2p - 1, \tag{10.80}$$

$$\frac{U_0}{k_0^{1/2}} = \frac{C_\mu p}{\sigma_k} = \frac{C_\mu(2p-1)}{\sigma_\varepsilon}, \tag{10.81}$$

and show that (for small x) convection and diffusion balance, with the dissipation terms being negligible in comparison. From Eq. (10.81) obtain

$$p = \frac{\sigma_k}{2\sigma_k - \sigma_\varepsilon} = \frac{1}{2-\sigma}, \tag{10.82}$$

where $\sigma \equiv \sigma_\varepsilon/\sigma_k$. Show that (for small x) k, ε, $L \equiv k^{3/2}/\varepsilon$, $\omega \equiv \varepsilon/k$, and ν_T vary as the following powers of x:

$$\frac{1}{2-\sigma}, \quad \frac{\sigma}{2-\sigma}, \quad \frac{\frac{3}{2}-\sigma}{2-\sigma}, \quad \frac{\sigma-1}{2-\sigma}, \quad 1, \tag{10.83}$$

respectively, and hence that all of these quantities are zero in the limit as x approaches zero provided that σ is between 1 and $1\frac{1}{2}$. Show that the speed of propagation of the turbulence front (relative to the mean flow) is

$$U_0 = \frac{1}{2\sigma_k - \sigma_\varepsilon}\left(\frac{\mathrm{d}\nu_T}{\mathrm{d}x}\right)_{x=0_+}. \tag{10.84}$$

10.11 Show that the k–ε model equations applied to the self-similar temporal mixing layer can be written

$$\frac{\partial k}{\partial t} = \frac{\partial}{\partial y}\left(\frac{C_\mu k^2}{\sigma_k \varepsilon}\frac{\partial k}{\partial y}\right) - \varepsilon\left(1 - \frac{\mathcal{P}}{\varepsilon}\right), \tag{10.85}$$

$$\frac{\partial \varepsilon}{\partial t} = \frac{\partial}{\partial y}\left(\frac{C_\mu k^2}{\sigma_\varepsilon \varepsilon}\frac{\partial \varepsilon}{\partial y}\right) - \frac{\varepsilon^2}{k}\left(C_{\varepsilon 2} - C_{\varepsilon 1}\frac{\mathcal{P}}{\varepsilon}\right). \tag{10.86}$$

With $\delta(t)$ being the width of the layer, the similarity variables are defined by

$$\xi \equiv \frac{y}{\delta}, \quad \hat{k}(\xi) \equiv \frac{k}{U_s^2}, \quad \hat{\varepsilon}(\xi) \equiv \frac{\varepsilon\delta}{U_s^3}, \tag{10.87}$$

where U_s is the (constant) velocity difference. Transform Eqs. (10.85) and (10.86) to obtain

$$-S\xi\frac{\mathrm{d}\hat{k}}{\mathrm{d}\xi} = \frac{\mathrm{d}}{\mathrm{d}\xi}\left(\frac{C_\mu \hat{k}^2}{\sigma_k \hat{\varepsilon}}\frac{\mathrm{d}\hat{k}}{\mathrm{d}\xi}\right) - \hat{\varepsilon}\left(1 - \frac{\mathcal{P}}{\varepsilon}\right), \tag{10.88}$$

$$-S\left(\hat{\varepsilon} + \xi\frac{\mathrm{d}\hat{\varepsilon}}{\mathrm{d}\xi}\right) = \frac{\mathrm{d}}{\mathrm{d}\xi}\left(\frac{C_\mu \hat{k}^2}{\sigma_\varepsilon \hat{\varepsilon}}\frac{\mathrm{d}\hat{\varepsilon}}{\mathrm{d}\xi}\right) - \frac{\hat{\varepsilon}^2}{\hat{k}}\left(C_{\varepsilon 2} - C_{\varepsilon 1}\frac{\mathcal{P}}{\varepsilon}\right), \tag{10.89}$$

where S is the spreading rate $S = U_s^{-1}\,\mathrm{d}\delta/\mathrm{d}t$.

Let ξ_e denote the edge of the turbulent region (so that k and ε are zero for $\xi \geq \xi_e$) and let x be the distance from the edge,

$$x \equiv \xi_e - \xi. \tag{10.90}$$

Show that the left-hand side of Eq. (10.88) can be written

$$-S\xi\frac{\mathrm{d}\hat{k}}{\mathrm{d}\xi} = S(\xi_e - x)\frac{\mathrm{d}\hat{k}}{\mathrm{d}x}. \tag{10.91}$$

Hence show that (for small x) the equations have the power-law solutions given in Exercise 10.10 ($k \sim x^p$ and $\varepsilon \sim x^q$).

10.4.3 Discussion

The k–ε model is arguably the simplest complete turbulence model, and hence it has the broadest range of applicability[2]. It is incorporated in most commercial CFD codes, and has been applied to a diverse range of problems including heat transfer, combustion, and multi-phase flows.

A discussion of its accuracy is deferred to the next chapter (Section 11.10), where its performance is compared with that of other turbulence models. Briefly; although it is usually acceptably accurate for simple flows, it can be quite inaccurate for complex flows, to the extent that the calculated mean flow patterns can be qualitatively incorrect. The inaccuracies stem from the turbulent-viscosity hypothesis and from the ε equation.

Also deferred to the next chapter (Section 11.7) is a discussion of near-wall treatments. Modifications to the standard k–ε model are required in order to apply it to the viscous near-wall region. For example, it may be seen from Fig. 10.3 that the appropriate value of C_μ decreases as y^+ decreases below 50.

The values of the standard k–ε model constants (Eq. 10.54) represent a compromise. For any particular flow it is likely that the accuracy of the model calculations can be improved by adjusting the constants. For decaying turbulence, $C_{\varepsilon 2} = 1.77$ (corresponding to the value of the decay exponent $n = 1.3$) is more suitable than $C_{\varepsilon 2} = 1.92$ (corresponding to the value of the decay exponent $n = 1.09$). A well-known deficiency of the k–ε model is that it significantly overpredicts the rate of spreading for the round jet. This problem can be remedied (for the round jet) by adjusting the value of $C_{\varepsilon 1}$ or $C_{\varepsilon 2}$. However, such *ad hoc* flow-dependent adjustments are of limited value. For a complete, generally applicable model, a single specification of the constants is required; and the standard values represent a compromise chosen (with subjective judgement) to give the 'best' performance for a range of flows.

Over the years, many 'modifications' to the standard k–ε model have been proposed, the usual motivation being to remedy poor performance for a particular class of flows. For example, Pope (1978) proposed an additional source term in the ε equation of the form $\bar{S}_{ij}\bar{\Omega}_{jk}\bar{\Omega}_{ki}k^2/\varepsilon$, so that the modified model yields the correct spreading rate for the round jet. Other modifications to the ε equation (based on $\bar{\Omega}_{ij}$) have been proposed by, for example, Hanjalić and Launder (1980) and Bardina, Ferziger, and Reynolds (1983). When these

[2] Recall from Section 8.3 that applicability does not imply accuracy.

modified models are applied to a range of flows, the general experience (Launder 1990, Hanjalić 1994) is that their overall performance is inferior to that of the standard model.

The model equation for ε has been presented here as being entirely empirical; but this is only one viewpoint. The renormalization group method (RNG) has been used to obtain the k–ε equation from the Navier–Stokes equations (see, e.g., Yakhot and Orszag (1986), Smith and Reynolds (1992), Smith and Woodruff (1998), and references therein). The values of the constants stemming from the RNG analysis are

$$C_\mu = 0.0845,\ C_{\varepsilon 1} = 1.42,\ C_{\varepsilon 2} = 1.68,\ \sigma_k = \sigma_\varepsilon = 0.72 \tag{10.92}$$

(Orszag *et al.* 1996), cf. Eq. (10.54). In the RNG k–ε model there is also an additional term in the ε equation, which is an *ad hoc* model, not derived from RNG theory. It is this term which is largely responsible for the difference in performance of the standard and RNG models.

10.5 Further turbulent-viscosity models

10.5.1 The k–ω model

Historically, many two-equation models have been proposed. In most of these, k is taken as one of the variables, but there are diverse choices for the second. Examples are quantities with dimensions of kL (Rotta 1951), ω (Kolmogorov 1942), ω^2 (Saffman 1970), and τ (Speziale, Abid, and Anderson 1992).

For homogeneous turbulence, the choice of the second variable is immaterial, since there is an exact correspondence among the various equations, and their forms are essentially the same (see Exercise 10.12). For inhomogeneous flows, the difference lies in the diffusion term. Consider, for example, the following model equation for $\omega \equiv \varepsilon/k$:

$$\frac{\bar{\mathrm{D}}\omega}{\bar{\mathrm{D}}t} = \nabla\cdot\left(\frac{\nu_\mathrm{T}}{\sigma_\omega}\nabla\omega\right) + C_{\omega 1}\frac{\mathcal{P}\omega}{k} - C_{\omega 2}\,\omega^2. \tag{10.93}$$

How does the k–ω model based on this equation differ from the k–ε model? One way to answer this question is to derive the ω equation implied by the k–ε model (see Exercise 10.13). Taking $\sigma_k = \sigma_\varepsilon = \sigma_\omega$ for simplicity, the result

$$\frac{\bar{\mathrm{D}}\omega}{\bar{\mathrm{D}}t} = \nabla\cdot\left(\frac{\nu_\mathrm{T}}{\sigma_\omega}\nabla\omega\right) + (C_{\varepsilon 1}-1)\frac{\mathcal{P}\omega}{k} - (C_{\varepsilon 2}-1)\omega^2 + \frac{2\nu_\mathrm{T}}{\sigma_\omega k}\nabla\omega\cdot\nabla k. \tag{10.94}$$

Table 10.2. *Values of C_{Z1} and C_{Z2} for various specifications of $Z = C_Z k^p \varepsilon^q$ (see Exercise 10.12)*

Z	p	q	C_{Z1}	C_{Z2}
k	1	0	1.0	1.0
ε	0	1	1.44	1.92
$\omega = \varepsilon/k$	−1	1	0.44	0.92
$\tau = k/\varepsilon$	1	−1	−0.44	−0.92
$L = k^{3/2}/\varepsilon$	$\frac{3}{2}$	−1	0.06	−0.42
$kL = k^{5/2}/\varepsilon$	$\frac{5}{2}$	−1	1.06	0.58
$\nu_T = C_\mu k^2/\varepsilon$	2	−1	0.56	0.08

Evidently, for homogeneous turbulence, the choices $C_{\omega 1} = C_{\varepsilon 1} - 1$ and $C_{\omega 2} = C_{\varepsilon 2} - 1$ make the models identical. However, for inhomogeneous flows, the k–ε model (written as a k–ω model) contains an additional term – the final term in Eq. (10.94).

The second most widely used two-equation model is the k–ω model that has been developed for over 20 years by Wilcox and others (see Wilcox (1993)). In this model, the expression for ν_T and the k equation are the same as those in the k–ε model. The difference lies in the use of Eq. (10.93) for ω rather than Eq. (10.53) for ε (or the implied ω equation, Eq. (10.94)). As described in detail by Wilcox (1993), for boundary-layer flows, the k–ω model is superior both in its treatment of the viscous near-wall region, and in its accounting for the effects of streamwise pressure gradients. However, the treatment of non-turbulent free-stream boundaries is problematic: a non-zero (non-physical) boundary condition on ω is required, and the calculated flow is sensitive to the value specified.

Menter (1994) proposed a two-equation model designed to yield the best behavior of the k–ε and k–ω models. It is written as a (non-standard) k–ω model, with the ω equation of the form of Eq. (10.94), but with the final term multiplied by a 'blending function.' Close to walls the blending function is zero (leading to the standard ω equation), whereas remote from walls the blending function is unity (corresponding to the standard ε equation). (The behavior of the k–ε model at a free-stream boundary has been analyzed by Cazalbou *et al.* (1994); see also Exercise 10.11.)

EXERCISES

10.12 Consider the quantity Z defined by

$$Z = C_Z k^p \varepsilon^q, \tag{10.95}$$

for given C_Z, p and q. From the standard k–ε model equations, show that, in homogeneous turbulence, the implied model equation for Z is

$$\frac{\mathrm{d}Z}{\mathrm{d}t} = C_{Z1}\frac{Z\mathcal{P}}{k} - C_{Z2}\frac{Z\varepsilon}{k}, \tag{10.96}$$

where

$$C_{Z1} = p + qC_{\varepsilon 1}, \tag{10.97}$$

$$C_{Z2} = p + qC_{\varepsilon 2}. \tag{10.98}$$

Hence verify the values of C_{Z1} and C_{Z2} in Table 10.2.

10.13 Given the standard k–ε model equations, show that the implied model equation for $\omega = \varepsilon/k$ is

$$\begin{aligned}\frac{\bar{\mathrm{D}}\omega}{\bar{\mathrm{D}}t} = \nabla\cdot\left(\frac{\nu_\mathrm{T}}{\sigma_\varepsilon}\nabla\omega\right) + (C_{\varepsilon 1}-1)\frac{\mathcal{P}\omega}{k} - (C_{\varepsilon 2}-1)\omega^2 \\ + C_\mu\left(\frac{1}{\sigma_\varepsilon}+\frac{1}{\sigma_k}\right)\frac{1}{\omega}\nabla\omega\cdot\nabla k \\ + C_\mu\left(\frac{1}{\sigma_\varepsilon}-\frac{1}{\sigma_k}\right)\left(\nabla^2 k + \frac{1}{k}\nabla k\cdot\nabla k\right).\end{aligned} \tag{10.99}$$

10.5.2 The Spalart–Allmaras model

Spalart and Allmaras (1994) described a one-equation model developed for aerodynamic applications, in which a single model transport equation is solved for the turbulent viscosity ν_T. Earlier proposals for such a model are described by Nee and Kovasznay (1969) and Baldwin and Barth (1990).

It is useful at the outset to appreciate the context of the development of the Spalart–Allmaras model. There is a natural progression in the models described above – algebraic, one-equation, two-equation – on to the Reynolds-stress models described in the next chapter. Each successive level provides a fuller description of the turbulence, and thereby removes a qualitative deficiency of its predecessor. If accuracy were the only criterion in the selection of models for development and application, then the choice would naturally tend toward the models with the higher level of description. However, as discussed in Section 8.3, cost and ease of use are also important criteria that favor the simpler models. It is useful, therefore, for model developers to work toward the best possible model at each level of description.

Arguably, a one-equation model for ν_T is the lowest level at which a model can be complete. Spalart and Allmaras (1994) developed the model to

remove the incompleteness of algebraic and one-equation models based on k, and yet have a model computationally simpler than two-equation models. The model is designed for aerodynamic flows, such as transonic flow over airfoils, including boundary-layer separation.

The model equation is of the form

$$\frac{\overline{\mathrm{D}}\nu_\mathrm{T}}{\overline{\mathrm{D}}t} = \nabla \cdot \left(\frac{\nu_\mathrm{T}}{\sigma_\nu} \nabla \nu_\mathrm{T} \right) + S_\nu, \tag{10.100}$$

where the source term S_ν depends on the laminar and turbulent viscosities, ν and ν_T; the mean vorticity (or rate of rotation) Ω; the turbulent viscosity gradient $|\nabla \nu_\mathrm{T}|$; and the distance to the nearest wall, ℓ_w. The details of the model are quite complicated: the reader is referred to the original paper which provides an enlightening account of the construction of the model to achieve particular desired behaviors.

In applications to the aerodynamic flows for which it is intended, the model has proved quite successful (see, e.g., Godin, Zingg, and Nelson (1997)). However, it has clear limitations as a general model. For example; it is incapable of accounting for the decay of ν_T in isotropic turbulence, it implies that, in homogeneous turbulence, ν_T is unaffected by irrotational mean straining; and it overpredicts the rate of spreading of the plane jet by almost 40%.

EXERCISE

10.14 Consider the Spalart–Allmaras model applied to high-Reynolds-number homogeneous turbulence. Argue that the laminar viscosity ν and the distance to the nearest wall ℓ_w are not relevant quantities. Hence show that dimensional and other considerations reduce Eq. (10.100) to

$$\frac{\mathrm{d}\nu_\mathrm{T}}{\mathrm{d}t} = S_\nu(\nu_\mathrm{T}, \Omega) = c_{\mathrm{b}1} \nu_\mathrm{T} \Omega, \tag{10.101}$$

where $c_{\mathrm{b}1}$ is a constant. Comment on the form of this equation for irrotational mean straining.

For self-similar homogeneous turbulent shear flow (in which Ω and $\mathcal{S}$ are equal), from the relation $-\langle uv \rangle = \nu_\mathrm{T}\, \partial \langle U \rangle / \partial y$, show that ν_T evolves by Eq. (10.101) with

$$c_{\mathrm{b}1} = \left(\frac{\mathcal{P}}{\varepsilon} - 1 \right) \left(\frac{\mathcal{S}k}{\varepsilon} \right)^{-1}. \tag{10.102}$$

Use experimental data (Table 5.4 on page 157) to estimate c_{b1} according to Eq. (10.102) and compare it with the Spalart–Allmaras value of $c_{\mathrm{b}1} = 0.135$.